

# Evaluation of *in vitro* bioactivity and biocompatibility of Bioglass<sup>®</sup>-reinforced polyethylene composite

J. HUANG\*, L. DI SILVIO†, M. WANG\*, I. REHMAN\*, C. OHTSUKI‡, W. BONFIELD\*

\**IRC in Biomedical Materials, Queen Mary and Westfield College, Mile End Road, London E1 4NS, UK*, †*IRC in Biomedical Materials, Institute of Orthopaedics, Royal National Orthopaedic Hospital, Brockley Hill, Stanmore, Middlesex HA7 4LP, UK*, ‡*Biomaterials Laboratory, Faculty of Engineering, Okayama University, Tsushima-Naka, Okayama-shi 700, Japan*

The bioactivity and biocompatibility of Bioglass<sup>®</sup>-reinforced high-density polyethylene composite (Bioglass<sup>®</sup>/HDPE) have been evaluated in simulated body fluid (SBF) and by *in vitro* cell culture, respectively. The formation of a biologically active hydroxy-carbonate apatite (HCA) layer on the composite surface after immersion in SBF was demonstrated by thin-film X-ray diffraction, infrared spectroscopy and scanning electron microscopy, indicating the *in vitro* bioactivity of Bioglass<sup>®</sup>/HDPE composites. The HCA layer was formed on the 40 vol % composite surface within 3 days immersion in SBF at a formation rate comparable to those on bioactive glass-ceramics, showing that *in vitro* bioactivity could be obtained in a composite. Furthermore, the composite was biocompatible to primary human osteoblast-like cells. In comparison with unfilled HDPE and tissue culture plastic control, a significant increase in cellular metabolic activity was found on the composite. Therefore, Bioglass<sup>®</sup>/HDPE composites have a promising biological response as a potential implant material.

## 1. Introduction

Bioglass<sup>®</sup> 45S5 is highly bioactive and is able to bond with natural tissue [1], but its brittle nature reduces its potential clinical applications. Various ductile composites which contain a bioactive, but brittle, ceramic or glass phase have been produced [2–6]. Bone formation on the composite surface *in vivo* has been observed [6–8] and the percentage of bone formed was related to the ceramic/glass content [8]. The effect of Bioglass<sup>®</sup> content on the *in vitro* bioactivity and biocompatibility of Bioglass<sup>®</sup>-reinforced high-density polyethylene (HDPE) composite (Bioglass<sup>®</sup>/HDPE) is reported in this paper.

A common characteristic of bioactive implants is the formation of a biologically active hydroxy-carbonate apatite (HCA) layer on their surfaces when implanted, which is thought to play an important role in the formation of direct bone bonding [1, 9]. *In vivo* studies are often difficult to interpret due to the complexity of various cell responses. *In vitro* studies provide a useful method for the initial screening of a material and can aid in understanding the performance of the material *in vivo*. The formation of an HCA layer on the surfaces of bioactive glasses and glass ceramics was also found

in physiological solutions [10–13]. For a material to be bioactive *in vivo*, it must have the ability to induce apatite formation on its surface *in vitro*. Therefore, the surface changes of Bioglass<sup>®</sup>/HDPE composites in a physiological solution have been investigated.

It is equally important to consider the changes in the local environment created by a composite which includes a highly reactive phase (i.e. Bioglass<sup>®</sup>) before *in vivo* testing of the material, as these changes may have considerable effects on the behaviour of the cells [14, 15]. Cytocompatibility is a basic requirement for an implant material. The simplicity, sensitivity and reliability of *in vitro* cell culture make it a useful initial screening method for biomaterials [16–18]. Furthermore, it is possible to test any toxic effect on human cells, thereby assessing the same cellular response as *in vivo*. In this work, primary human osteoblast-like (HOB) cells have been used to study the cellular response to Bioglass<sup>®</sup>/HDPE composites.

## 2. Materials and methods

Bioglass<sup>®</sup>/HDPE composite was produced by incorporation of Bioglass<sup>®</sup> 45S5 (US Biomaterials Co.)

\*Author to whom all correspondence should be addressed.

Selected paper from the 13th European Conference on Biomaterials, Göteborg, Sweden.

particles into HDPE (Rigidex HM4560EP, BP Chemicals Ltd) through blending, compounding and compression moulding [4]. The median particle size of Bioglass<sup>®</sup> used in this study was 56  $\mu\text{m}$  with volume percentages of Bioglass<sup>®</sup> in the composite of 20% and 40%. The specimens ( $10 \times 10 \text{ mm}^2$ ) were cut from composite plate and polished down to 1  $\mu\text{m}$  with diamond paste, then cleaned in an ultrasonic bath in ethanol and stored in a desiccator until analysis.

### 2.1. Preparation of simulated body fluid

Simulated body fluid (SBF K9) was used as it contains inorganic ion concentrations close to those in blood plasma [10] and was prepared by dissolving reagent-grade chemicals of sodium chloride (NaCl), sodium hydrogen carbonate ( $\text{NaHCO}_3$ ), potassium chloride (KCl), dipotassium hydrogen phosphate ( $\text{K}_2\text{HPO}_4 \cdot 3\text{H}_2\text{O}$ ), magnesium chloride hexahydrate ( $\text{MgCl}_2 \cdot 6\text{H}_2\text{O}$ ), calcium chloride dihydrate ( $\text{CaCl}_2 \cdot 2\text{H}_2\text{O}$ ), sodium sulfate ( $\text{Na}_2\text{SO}_4$ ) and tris-(hydroxymethyl) aminomethane, into distilled water and buffered to pH 7.25 at 37 °C with hydrochloric acid (HCl).

Specimens with the ratio of specimen surface area to solution volume of  $10 \text{ mm}^2 \text{ ml}^{-1}$  were immersed in SBF K9 at 37 °C for various periods. The changes of the surface were analysed by various techniques.

### 2.2. Thin-film X-ray diffraction (TF-XRD)

TF-XRD was carried out on a Siemens D5000 diffractometer using  $\text{CuK}_{\alpha 1}$  radiation in detector scan mode with a thin-film analyser. Samples were aligned at 1° to the incident beam. A step size of 0.02° ( $2\theta$ ) and a scan time of 5 s were used and data were collected from 20° to 50°.

### 2.3. Fourier transform–infrared spectroscopy (FT–IR)

A Nicolet 800 Fourier transform–infrared spectrophotometer equipped with an attenuated total reflectance (ATR) objective was used to analyse the changes of the composite surface after immersion in SBF, detecting the appearance of ionic groups, such as phosphate and carbonate. FT–IR spectra were collected over the range of  $4000\text{--}650 \text{ cm}^{-1}$ , with the resolution of 4 wave number.

### 2.4. Scanning electron microscopy (SEM)

The surface of the composite was coated with a thin layer of gold before examination in a Jeol 6300F field-emission SEM at an accelerating voltage of 5 keV. When the elemental composite was analysed, the composite surface was coated with carbon and examined using a conventional Jeol 6300 SEM with an energy-dispersive X-ray analysis (EDX) attachment. The distribution of the element on the composite surface was obtained by line scanning or mapping.

## 2.5. Cytotoxicity

The initial cytotoxicity tests for the composite were performed on extracts prepared by elution of the test samples in Dulbecco's modified Eagle's medium (DMEM) supplemented with 10% foetal calf serum (FCS), at 37 °C for 24 h. Tissue culture plastic (TcP) and polyvinylchloride (PVC) were used as non-toxic and as toxic controls, respectively. The cell viability was assessed using the 3-(4,5-dimethylthiazol-2-yl)-2,5-diphenyltetrazolium bromide (MTT) assay due to its sensitivity [19]. This assay measures intracellular mitochondrial activity of the cells, which involves reduction of MTT by intracellular dehydrogenases of viable cells to a blue formazan. Reduction of MTT occurs if cells have a significant level of oxidative metabolism.

A primary human osteoblast-like (HOB) cell culture model was used [17]. HOB cells were cultured in the extracts at 37 °C in a humidified air with 5%  $\text{CO}_2$  for 24 h, followed by a further 4 h incubation in the presence of 10% MTT (Sigma, UK). The medium was then removed and replaced with dimethyl sulfoxide (Merck, UK) and mixed for 10 min to ensure complete dissolution of crystals. Absorbance was measured on a Dynatech MR 700 microplate reader, using a test wavelength of 570 nm and a reference wavelength of 630 nm.

## 3. Results

### 3.1. TF-XRD

Fig. 1 shows the TF-XRD patterns of the 40% composite before and after immersion in SBF. The formation of an apatite layer on the composite surface was first observed after 3 days in SBF, with one apatite peak at approximately 26° ( $2\theta$ ) and another between 31° and 33° appearing on the XRD pattern. The intensity of apatite peaks compared with those of HDPE peaks increased with time and another peak at 49° appeared after 4 week immersion, indicating the formation and growth of an apatite layer on the composite surface in SBF.

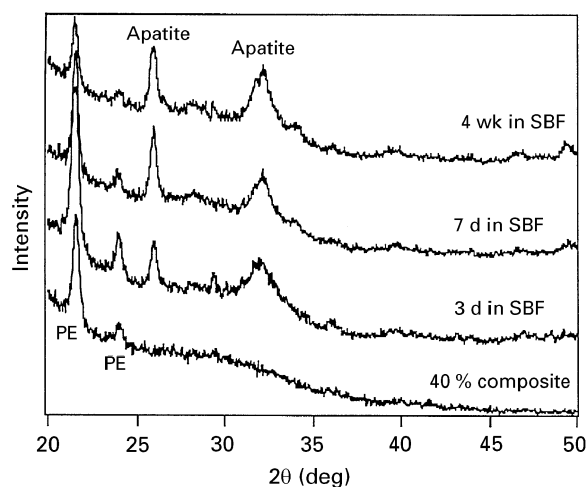


Figure 1 TF-XRD patterns of 40% Bioglass<sup>®</sup>/HDPE composite before and after 3 days, 7 days and 4 weeks immersion in SBF.

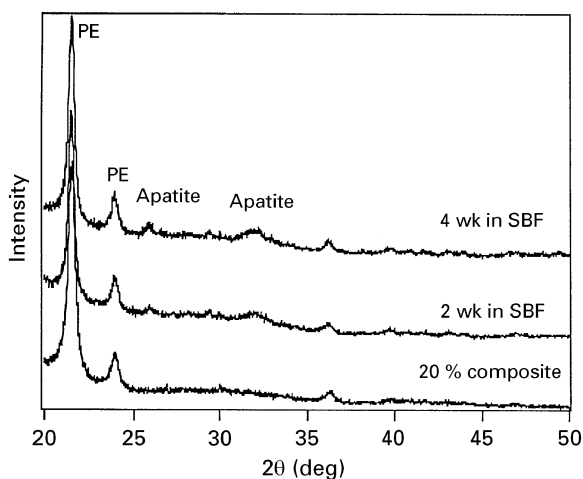


Figure 2 TF-XRD patterns of 20% Bioglass<sup>®</sup>/HDPE composite before and after 2 and 4 weeks immersion in SBF.

The TF-XRD pattern of the 20% composite before immersion was similar to that of the 40% composite. Broad apatite peaks were noted after 2 weeks and their intensity slightly increased after 4 weeks in SBF (Fig. 2).

### 3.2. FT-IR

FT-IR spectra of the composite before immersion consisted of CH<sub>2</sub> vibrations from HDPE and Si-O vibrations from Bioglass<sup>®</sup>. For the 40% composite, after immersion in SBF, the intensity of the Si-O vibration mode decreased, a week phosphate peak appeared after 2 h and the peak intensity increased with immersion time (Fig. 3). A small carbonate peak at 872 cm<sup>-1</sup> appeared with a sharp phosphate peak after 3 days and the intensity of the phosphate peak increased continuously. Other carbonate peaks at 1415 and 1454 cm<sup>-1</sup> were observed after 7 days in SBF, showing the incorporation of carbonate in the structure of apatite, which is similar to bone mineral apatite. Simultaneously, the intensity of CH<sub>2</sub> vibration peaks decreased until they were totally masked by the surface apatite layer.

The changes occurring on the 20% composite after immersion in SBF were similar to, but relatively slower than, those on the 40% composite (Fig. 4). The formation of apatite on the composite surface was confirmed by the appearance of phosphate as well as carbonate peaks. The phosphate peak intensity compared with those of CH<sub>2</sub> vibration increased with time. However, the apatite formed was insufficient to mask the HDPE matrix, which resulted in the existence of moderate CH<sub>2</sub> vibration peaks in the FT-IR spectra.

### 3.3. SEM

Bioglass<sup>®</sup> particles were evenly distributed in HDPE matrix before immersion in SBF. The amount of Bioglass<sup>®</sup> on the surface of the composite increased with content (Fig. 5). The reaction of Bioglass<sup>®</sup> particles with the solution started immediately after immersion of the composite in SBF. The silanol,

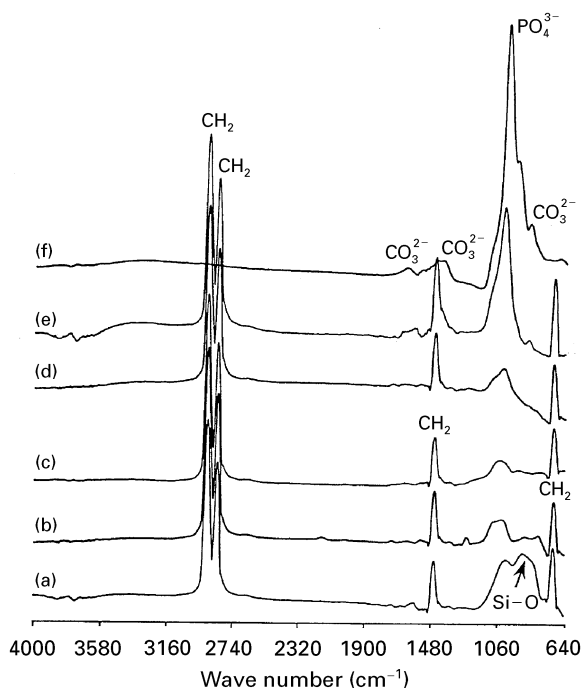


Figure 3 FT-IR spectra of 40% Bioglass<sup>®</sup>/HDPE composite (a) 0 h, (b) 2 h, (c) 8 h, (d) 16 h, (e) 3 days and (f) 7 days in SBF.

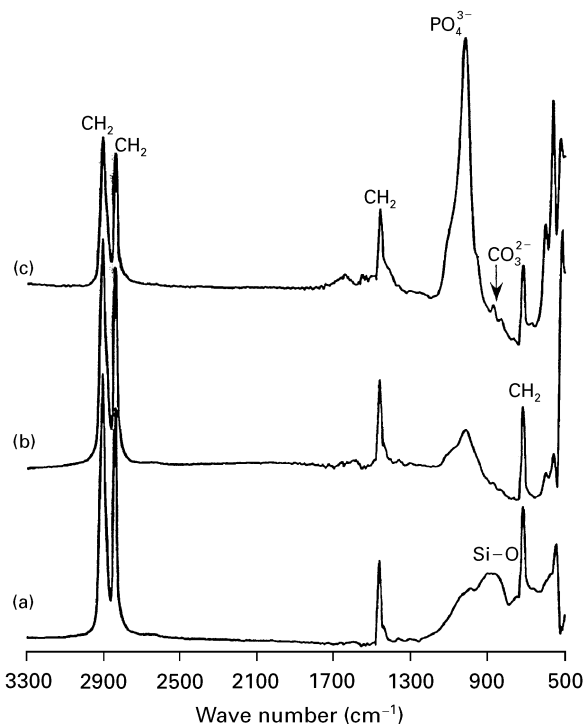


Figure 4 FT-IR spectra of 20% Bioglass<sup>®</sup>/HDPE composite (a) 0 h, (b) 2 days, and (c) 2 weeks in SBF.

resulting from the initial leaching, provided sites for apatite nucleation, from which the apatite crystals grew until the whole particle was covered by apatite. After covering Bioglass<sup>®</sup> particles, the apatite may or may not spread over the PE matrix, depending on the volume content of Bioglass<sup>®</sup> particles in the composite. For the 40% composite, the apatite was found on the PE matrix as well as on Bioglass<sup>®</sup> particles in comparison, the apatite localized around the Bioglass<sup>®</sup> particles on the 20% composite (Fig. 6).

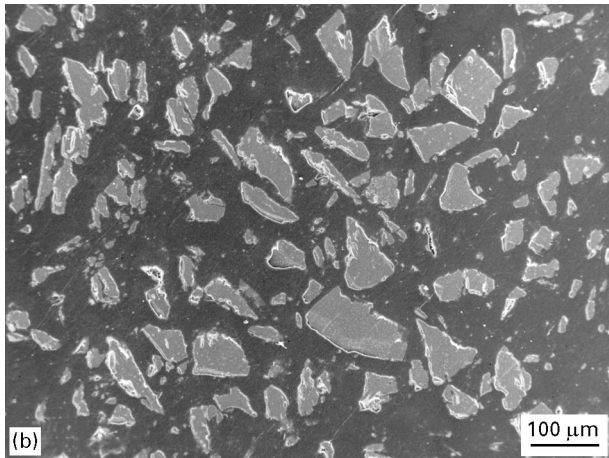
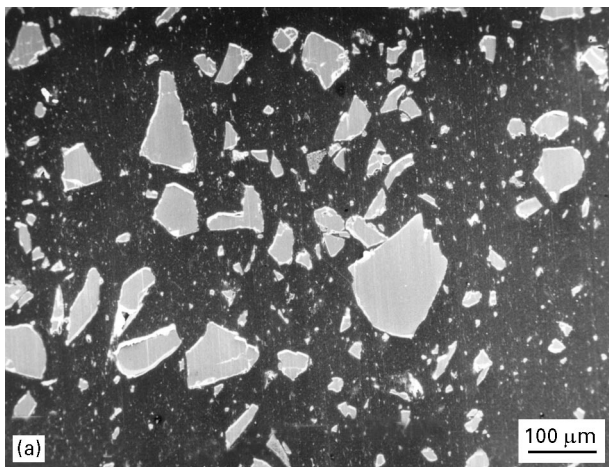


Figure 5 Scanning electron micrograph of polished surface of (a) 20% and (b) 40% Bioglass<sup>®</sup>/HDPE composite.

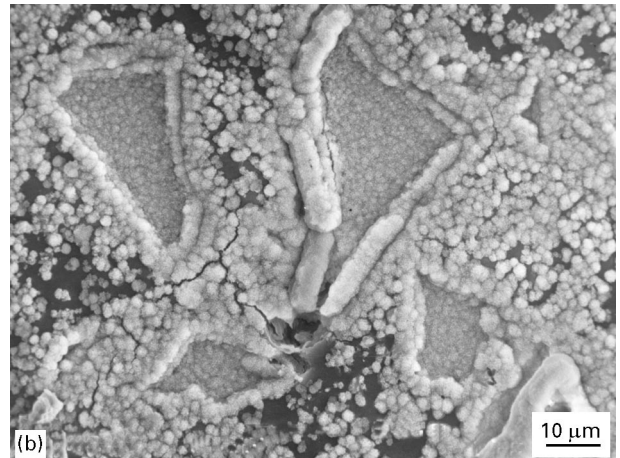
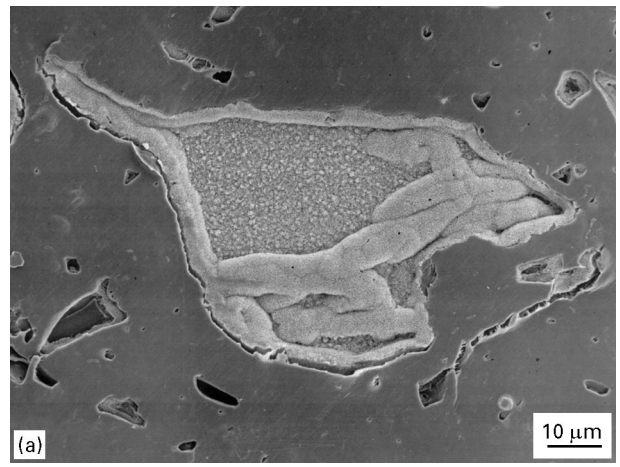


Figure 6 Formation of HCA layer on (a) 20% and (b) 40% Bioglass<sup>®</sup>/HDPE composite after 7 days in SBF.

### 3.4. Cytotoxicity

The viability of HOB cells after 24 h culture in the extracts is indicated in Fig. 7. None of the test materials released any ‘toxic leachables’ during 24 h elution. The cellular activity on PE was within the same range as that on the non-toxic control Tcp, while a significant increase in cellular metabolic activity was found on both composites ( $p < 0.001$ ).

## 4. Discussion

Formation of a biologically active HCA layer on the surfaces of Bioglass<sup>®</sup>/HDPE composite after immersion in SBF was found from TF-XRD, FT-IR analysis and SEM examination, indicating the *in vitro* bioactivity of the composite.

Previous work has shown that the reaction with SBF of individual micrometre-sized Bioglass<sup>®</sup> particles in the composite was similar to that of bulk Bioglass<sup>®</sup> [20]. The silanol formed from the early ion exchange and leaching provides a favourable site for nucleation and growth of the apatite. It was found that, the number of nucleation sites and thus the apatite formation rate were proportional to the Bioglass<sup>®</sup> content. The HCA layer was formed on

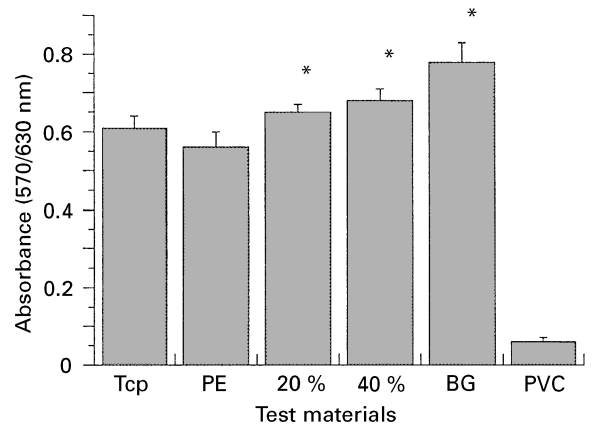


Figure 7 Viability of HOB cells following 24 h exposure to 24 h eluted media from test and control materials, statistically significant differences from Tcp using Student’s *t*-test indicated by \* $p < 0.001$ .

the 40% composite surfaces within 3 days in SBF. Such a fast apatite formation rate is comparable with that on Bioglass<sup>®</sup> and other bioactive glass ceramics [10], showing that high *in vitro* bioactivity was obtained on the composite. While the formation rate was slower with a decreased Bioglass<sup>®</sup> content, such as in the 20% composite, the ability to induce apatite formation did not change on Bioglass<sup>®</sup> particles in the composite.

One advantage of Bioglass<sup>®</sup> 45S5 is its high bioactivity, which promotes bonding to soft tissue as well as to hard tissue. However, the high bioactivity of Bioglass<sup>®</sup> 45S5 did not lead to the highest interfacial failure strength of Bioglass<sup>®</sup> implants [21], probably due to the formation of a thick silicon-gel layer. Al<sub>2</sub>O<sub>3</sub> was introduced into the glass composition to reduce the thickness of the silicon-rich layer, but it reduced the bioactivity of the glass [22]. By introducing Bioglass<sup>®</sup> 45S5 particles into HDPE matrix, the high bioactivity of Bioglass<sup>®</sup> can be retained, but controlled, in the composite, which is an advantage of this approach.

Furthermore, no cytotoxic effect was observed for the composite, and in addition a significant increase in cellular activity was found, suggesting that the Bioglass<sup>®</sup> in the composite was able to stimulate cellular activity by creating a favourable microenvironment for cell proliferation and growth. It was shown that sodium, calcium, phosphorus and silicon ions were released from Bioglass<sup>®</sup> 45S5 through a series of surface reactions [11], but the effect of releasing these ions into the surrounding medium has not yet been established. This study showed that any leachables that may have been present in the 24 h extracts did not have a detrimental effect on HOB cell activity, but, an increase in cell mitochondrial activity was observed. This "stimulation" effect may be related to the release of soluble silicon, which has been reported to play an active role on bone formation and calcification [23]. The relation between silicon concentration and HOB cell activity remains to be elucidated.

## 5. Conclusion

Bioglass<sup>®</sup>/HDPE composite is bioactive and biocompatible and has a stimulatory effect on HOB cells *in vitro*. These properties can be optimized by composite formulation and hence, the composite is a potential implant material for variety of applications.

## Acknowledgements

The financial support from US Biomaterials for this project and the continuing support of EPSRC for the IRC core programme are gratefully acknowledged.

## References

1. L. L. HENCH, *J. Amer. Ceram. Soc.* **74** (1991) 1487
2. W. BONFIELD, M. D. GRYNPAS, A. E. TULLY, J. BOWMAN, J. ABRAM, *Biomaterials* **2** (1981) 185.
3. P. DUCHEYNE and L. L. HENCH, *J. Mater. Sci.* **17** (1982) 595.
4. M. WANG, W. BONFIELD and L. L. HENCH, *Bioceramics* **8** (1995) 383.
5. R. L. OREFICE, G. P. LATORRE, J. K. WEST and L. L. HENCH, *ibid.* **8** (1995) 409.
6. W. BONFIELD, C. DOYLE and K. E. TANNER, in "Biological and Biomechanical Performance of Biomaterials", edited by P. Cristel, A. Meunier and A. J. C. Lee (Elsevier, Amsterdam, 1986) p. 153.
7. P. DUCHEYNE, M. MARCOLONGO and E. SCHEPERS, in "An Introduction to Bioceramics" edited by L. L. Hench and J. Wilson (World Scientific, Singapore, 1993) p. 281.
8. J. TAMNRA, K. KAWANABE, M. KOBAYASHI, T. NAKAMURA, T. KOKUBO, S. YOSHIHARA and T. SHIBUYA, *J. Biomed. Mater. Res.* **30** (1996) 85.
9. T. KITSUGI, T. YAMAMURO, T. NAKAMURA, S. HIGASHI, Y. KAKUTANI, K. HYAKUNA, S. ITO, T. KOKUBO, M. TAKAGI and T. SHIBUYA, *ibid.* **20** (1986) 1295.
10. T. KOKUBO, H. KUSHITANI, S. SAKKA, T. KITSUGI and T. YAMAMURO, *ibid.* **24** (1990) 721.
11. L. L. HENCH and G. P. LATORRE, *Bioceramics* **5** (1992) 67.
12. M. R. FILGUEIRAS, G. LATORRE and L. L. HENCH, *J. Biomed. Mater. Res.* **27** (1993) 445.
13. C. OHTSUKI, Y. AOKI, T. KOKUBO, Y. BANDO, M. NEO and T. NAKAMURA, *J. Ceram. Soc. Jpn* **103** (1995) 449.
14. U. GROSS, H. J. SCHMITZ, R. KINNE, F. R. FENDLER and V. STRUNZ, in "Biomaterials and Clinical Application", edited by A. Pizzoferrato, P. G. Marchetti, A. Ravaglioli and A. J. C. Lee (Elsevier, Amsterdam, 1987) p. 547.
15. A. EI-GHANNAM, P. DUCHEYNE and I. SHAPIRO, *Bioceramics* **6** (1993) 143.
16. W. C. A. VROUWENVELDER, C. G. GROOT and K. DE GROOT, *Biomaterials* **13** (1992) 382.
17. L. DI SILVIO, PhD thesis, University of London (1995).
18. A. A. IGNATIUS and L. E. CLAES, *Biomaterials* **17** (1996) 831.
19. C. J. CLIFFORD and S. DOWNES, *J. Mater. Sci. Mater. Med.* **7** (1996) 637.
20. J. HUANG, M. WANG, I. REHMAN, J. KNOWLES and W. BONFIELD, *Bioceramics* **8** (1995) 389.
21. T. YAMAMURO, in "An Introduction to Bioceramics" edited by L. L. Hench and J. Wilson (World Scientific, Singapore, 1993) p. 89.
22. O. H. ANDERSSON, J. ROSENQVIST and K. H. KARLSSON, *J. Biomed. Mater. Res.* **27** (1993) 941.
23. L. L. HENCH, *Bioceramics* **7** (1994) 3.

Received 5 May

and accepted 12 May 1997